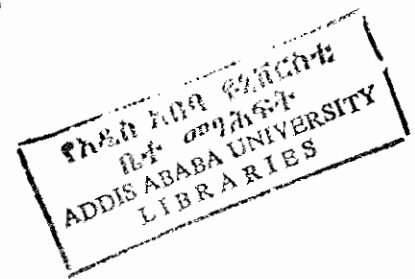


ADDIS ABABA UNIVERSITY
SCHOOL OF GRADUATE STUDIES

MEAN FIELD THEORY OF FERROELECTRICITY
IN LIQUID CRYSTALS



TEREFE GETANEH

JUNE 2000

**MEAN FIELD THEORY OF FERROELECTRICITY
IN LIQUID CRYSTALS**

A Thesis Presented to the
School of Graduate Studies
Addis Ababa University

In partial fulfilment of
the requirements for the Degree of
Master of Science in Chemistry

By

Terefe Getaneh

June, 2000

ADDIS ABABA UNIVERSITY
SCHOOL OF GRADUATE STUDIES

MEAN FIELD THEORY OF FERROELECTRICITY
IN LIQUID CRYSTALS

By

Terefe Getaneh

Department of Chemistry

Faculty of Science

Approved by Examining Board:

Dr. Habtamu Zewdie
Advisor

Habtamu Zewdie

Prof. Theodros Solomon
Examiner and Coordinator

Theodros Solomon

Dr. Bernd Hundhammer
Examiner

Bernd Hundhammer

Dr. Mulgeta Bekele
Examiner

Mulgeta Bekele

Acknowledgment

I am grateful to my supervisor, Dr. Habtamu Zewdie, for his consistent supervision and for the time he has devoted in explaining the new concepts in my research area without any reservation. I would also like to express my deep appreciation to him for the interest I got in liquid crystals starting from my undergraduate years.

It is my pleasure to express my heartfelt gratitude to Dr. Wendimagegn Mammo for his unreserved cooperation, encouragement and fatherly advice, and Prof. Theodoros Solomon for his material support.

I would like to acknowledge the Department of Chemistry, Addis Ababa University, for allowing me to do MSc study and for the time I am allowed to use for the study.

Finally, my special acknowledgement goes to the German Academic Exchange Service (Deutscher Akademischer Austauschdienst/DAAD) for the financial support through the In-Country Scholarship Award.

.....
.....
.....
.....
.....
.....
.....
.....
.....
.....

Table of Contents

	pages
Abbreviations and symbols	i
List of Tables	iii
List of Figures	iv
Absrtact	v
1. Introduction	1
1.1 Classification of Liquid Crystals Based on Degree of Order	2
1.2 Ferroelectricity in Liquid Crystals	5
2. Objectives of the Project	8
3. Significance of the Study	8
4. Mean Field Theory of Nematic Liquid Crystals	9
4.1 Thermodynamics of the Nematic Phase	14
5. Mean Field Theory of Ferroelectricity in Nematic Liquid Crystals	19
5.1 Effect of Pure Dipolar Interaction on Nematics	23
5.2 Effect of Coupling Terms on Nematics	28
5.3 Phase diagrams Using Different Potential Models	31
6. Conclusion	35
References	36
Appendix	38

Abbreviations and Symbols

LCD	liquid crystal display
I	isotropic
N	nematic
FN	ferroelectric-nematic
NI	nematic to isotropic
$P_1(\cos\theta)$	first order legendre polynomial
$P_2(\cos\theta)$	second order legendre polynomial
$\langle P_1 \rangle$	average of first order legendre polynomial (ferroelectric order parameter)
$\langle P_2 \rangle$	average of second order legendre polynomial (ordinary nematic order parameter for cylindrically symmetric molecules)
\hat{n}	a unit vector which represent the average direction of long molecular axis of rod-like molecules in a nematic phase
θ	an angle between the molecular axis and the director
$V(\cos\theta)$	single molecule orientational potential energy (mean field potential)
V_{\min}	the minimum value of the potential on the potential versus orientational angle curve
ε	potential well that measures the overall strength of intermolecular interaction
f	orientational distribution function
k	Boltzmann's constant

T	absolute temperature
T*	reduced temperature
Z	single molecule partition function
E	internal energy
N	number of molecules
$\langle V \rangle$	average value of potential
S	entropy
A	Helmholtz free energy
E*	reduced internal energy
S*	reduced entropy
A*	reduced Helmholtz free energy
ΔE^*	nematic to isotropic transitional reduced internal energy
ΔS^*	nematic to isotropic transitional reduced entropy
ΔA^*	nematic to isotropic transitional reduced Helmholtz free energy
T^*_{NI}	nematic to isotropic transition reduced temperature
λ	a coefficient for pure first rank order parameter
δ	a coefficient for coupling terms (coupling between first rank and second rank order parameters)
λ_c and δ_c	critical point values of λ and δ
λ_{tr} and δ_{tr}	triple point values of λ and δ

List of Tables

	pages
Values of the reduced temperature and order parameters at the critical values of λ and δ	32
Values of the reduced temperature and order parameters at the triple point values of λ and δ	32

List of Figures

	Pages
Schematic representation of nematic order isotropic phase	2
Schematic representation of cholesteric order	3
Schematic representation of smectic A and Smectic B orders	4
Coordinate system to define orientation of a uniaxial molecule in a laboratory frame	10
Orientation dependence of mean field potential	11
Orientation dependence of distribution function	12
Temperature dependence of $\langle P_2 \rangle$	13
Temperature dependence of free energy near transition	15
Equilibrium order parameter as a function of reduced temperature	16
Behaviour of internal energy and heat capacity for first and second order phase transitions.....	17
Orientation dependence of various potentials	21
Ferroelectric-nematic (FN),nematic (N) and isotropic regions on the order parameters versus reduced temperature plot for potential d	24
Behaviour of $\langle P_1 \rangle$ and $\langle P_2 \rangle$ at different values of λ for potential d	26
Phase diagram for potential d	27
Temperature dependence of $\langle P_1 \rangle$ and $\langle P_2 \rangle$ for various potential models	29
Phase diagrams for various potential models	31

Abstract

Using mean field potential containing the lowest symmetry allowed first rank, second rank and coupling of the two terms, we have studied the ferroelectricity in nematic liquid crystals. By taking various combinations of the terms, we have designed a number of potential models and performed mean field calculations for each potential. The significance of a pure dipolar and coupling interaction terms are investigated. The pure dipolar interaction term has been found to show more influence than the coupling terms for the formation of ferroelectricity in nematic liquid crystal. Phase diagrams that show ferroelectric-nematic (FN), nematic (N) and isotropic phases are produced for the various potential models.

1. Introduction

The tradition that matter exists only in three states (solid, liquid and gas) is not always correct. Because there are a number of organic materials that do not show a single transition from solid to liquid. Instead, they show a series of transitions involving new phases whose mechanical and optical properties are intermediate between those of a liquid and those of a crystal. For these reason, these new phases are called liquid crystals or 'mesomorphic phases' (or simply 'mesophases') to mean intermediate phases.

The constituent molecules in a crystal are regularly stacked, i.e., their centers of gravity are located on a three dimensional periodic lattice whereas in a liquid the centers of gravity are randomly distributed in space. The molecular ordering in the liquid crystals lies between that of a crystal and that of an isotropic liquid. The partial ordering of the molecules may be either translational or rotational or both. Obviously, translational order can be realized regardless of molecular shape whereas rotational order has meaning only when the constituent molecules are elongated (nonspherical). Hence, molecular structure is an important factor in determining the kind and extent of ordering. The molecules that form liquid crystals are more or less elongated in shape.

Research in the field of high technology materials is changing the world for the better. One such materials is liquid crystals. Nowadays everyone frequently encounters with liquid crystal displays (LCDs) in wristwatches, calculators, and information displays. Research in the application of LCDs for television screens are expected to revolutionize the way we watch TV [1]. Liquid crystals are also very useful in medicine as thermographs to detect cancer on

a skin surface, in NMR as solvents for determination of molecular structure, and in information technology to make high capacity storage device [2].

1.1 Classification of Liquid Crystals Based on Degree of Order

Liquid crystals can be classified into various types according to their degree of order. This classification is a scheme based primarily upon their symmetry. This scheme, first proposed by Friedel [3,4], distinguishes three major classes: the nematic, the cholesteric and the smectic phases.

i. Nematic Liquid Crystal

This is the most commonly occurring liquid crystal and has the lowest degree of order from all the liquid crystals. In the nematic phase, the molecules tend to align parallel to each other and hence there is long range orientational order, however, there is no long range correlation of the molecular center of gravity positions, Fig. 1. From this figure we see that the difference of the nematic phase from the isotropic phase is only in orientational order, i.e., the long molecular axes in the nematic phase are directed along a preferred axis on the average. The unit vector that represent this preferred direction is called director and denoted by a symbol \hat{n} .

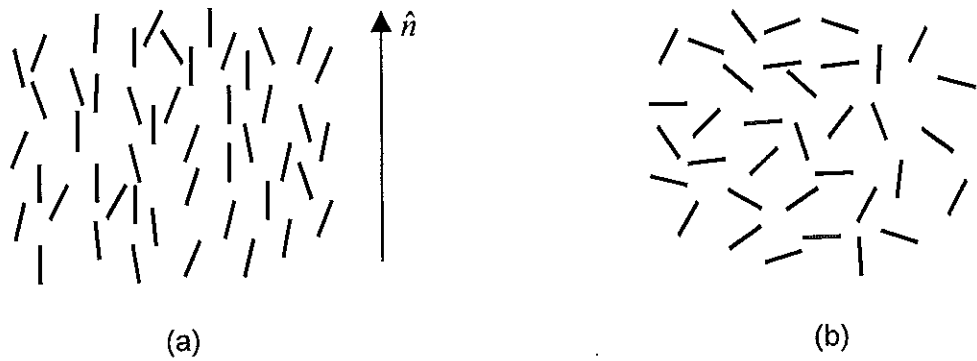


Fig. 1 Schematic representation of (a) nematic order and (b) isotropic phase.

ii. Cholesteric Liquid Crystal

This is a distorted form of the nematic phase. If a chiral molecule is dissolved in a nematic liquid, the structure undergoes a helical distortion. Locally, the cholesteric phase is very similar to a nematic phase. The centers of gravity have no long range order, and the molecular orientation shows a preferred axis. However, the preferred axis is not constant in space rather it forms a helical conformation along a helical axis, Fig. 2.

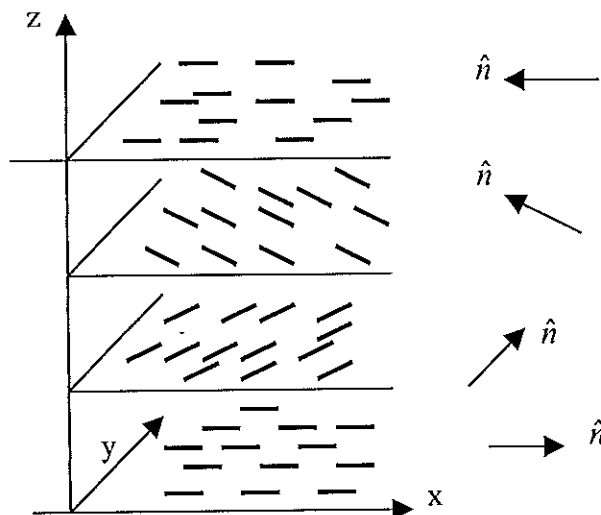


Fig. 2 Schematic representation of cholesteric order.

iii. Smectic Liquid Crystals

According to the various degree of order and the symmetries present, the smectic phase is further sub-divided as smectic A, smectic C, smectic B, etc. If we take the smectics A, C and B, they have one common feature, i.e., all the three have one degree of translational ordering, resulting in a layered structure.

a. Smectic A

Within the layers of a smectic A phase the molecules are on the average aligned parallel to the layer normal and have no long range order with respect to center of gravity position. Hence, each layer is a two dimensional liquid. The layer thickness is close to the full molecular length, Fig. 3a.

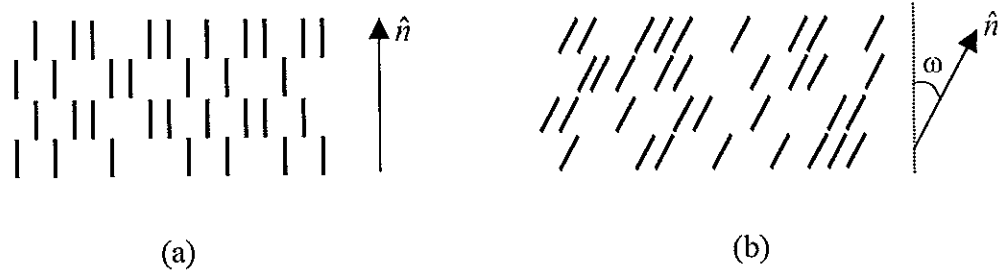


Fig. 3 Schematic representation of (a) smectic A order, and (b) smectic C order. ω is the tilt angle from the layer normal.

b. Smectic C

In smectic C, each layer is still a two-dimensional liquid. The layer thickness is significantly less than the molecular length. This has been interpreted as evidence for a uniform tilting of the molecular axis with respect to the layer normal, Fig. 3b.

c. Smectic B

In addition to the layered structure, there is ordering of the constituent molecules within the layers of the smectic B phase. Hence, the layers appear to have the periodicity and rigidity of a two-dimensional solid. However, the mechanical properties of the smectic B phase are quite different from those that would be expected for a material having full three-dimensional order.

1.2 Ferroelectricity in Liquid Crystals

A substance is called ferroelectric when it possesses spontaneous electric polarization such that the polarization can be reversed by an electric field [5-7]. The name ferroelectricity refers to certain magnetic analogies, though it is somewhat misleading in that there is no connection with iron (ferrum) at all. According to dipole theory of ferroelectricity [5], the existence of spontaneous polarization in general requires a physical model in which the dipole moments of the different unit cells or molecules are oriented along a common

direction. The dipole moment per unit cell or molecule may result partly from electronic and ionic displacements and partly from permanent dipoles.

It is curious enough that the contribution of polar interactions be normally neglected even though one of the first theories put forward on the structure of liquid crystals attribute the forces responsible for liquid crystal orientation ordering to polar forces [8]. This hypothesis was later proved unsatisfactory as a general ordering mechanism, because no macroscopic dipole ordering is observed in nematic and, even more stringently, because apolar nematic were synthesized [9,10]. Indeed such a great variety of different liquid crystals have now been prepared that the hypothesis of collective ordering effects being due to a combination of different interactions both steric and attractive rather than to a single ubiquitous one has become a very plausible proposition [11,12]. On the other hand, although dipoles may not be determinant for the existence of an ordered phase, they are nevertheless present in great majority of nematogens and they will produce some effect [13-16].

A number of molecules (mesogens) that form liquid crystal phases have symmetries consistent with the formation of ferroelectric phases and nonzero electric dipole moments. Furthermore, there is no fundamental reason that ferroelectric phases should not exist. However, only the chiral smectic liquid crystals have been observed to be ferroelectric [17,18]. The thermodynamic properties of chiral antiferroelectric (smectic C_A^*), ferroelectric (smectic C^*), and intermediate phases (smectic C_α^* , smectic C_γ^*) of chiral smectic liquid crystals have recently attracted a lot of attention. The reason for this is the extraordinary optical and electro-optical properties of these novel phases that have a great potential for application in flat panel displays. Ferroelectric liquid crystals have become also interesting

for their fundamental properties. It is, therefore, interesting to develop simple molecular models that try to find out the key ingredients that could give ferroelectric liquid crystals [19-21].

By constructing an effective single particle Hamiltonian for a simple model, Palffy-Muhoray *et al* [13] have examined the possibility that molecules with permanent dipole moments can form a ferroelectric nematic (FN) phase. They have shown that reasonable electric dipole interactions between disk-shaped molecules may lead to such a phase, and calculate the phase diagram using mean field-theory. In their Hamiltonian, they have included terms which are couplings of ferroelectric and usual nematic order parameters and have studied the effects of the terms as a whole. However, they have not included a pure dipolar interaction term and have not investigated the significance of the various terms in the potential.

In this work we will include a pure dipolar interaction term as well as couplings of the ferroelectric and the usual nematic order parameters. We will use the average of the first order Legendre polynomial (first rank term) as the ferroelectric order parameter and the average of the second order Legendre polynomial (second rank term) as usual nematic order parameter for cylindrically symmetric molecules. Therefore, a pure first rank term will be used to represent pure dipolar interaction and terms which are couplings of the first and the second rank terms represent couplings of ferroelectric and usual nematic order parameters.

To investigate the significance of the various terms in our potential model, we will construct different potential models and investigate the behaviour of the ferroelectric and nematic

order parameters for each potential model by doing mean field calculation. Finally, phase diagrams for all potential models that include the first and second rank terms will be produced. The ferroelectric-nematic (FN), nematic (N) and isotropic (I) phases will be shown on the phase diagrams.

2. OBJECTIVES OF THE PROJECT

1. To develop and investigate the simplest symmetry allowed hamiltonian for meanfield studies of ferroelectric liquid crystals.
2. To carry out an extensive studies on the Hamiltonian and investigate the behaviour of ferroelectric and usual nematic order parameters.
3. To study the significance of the various interaction terms included in the potential.
4. To provide phase diagrams which could be used as a reference to carry out detailed computer simulation studies.

3. SIGNIFICANCE OF THE STUDY

1. Mean field studies are essential to explore the value of a model Hamiltonian for studies of liquid crystals.
2. Molecular field studies enable us to discover the various thermodynamically stable liquid crystal phases and identify their structure and range of stabilities.
3. We use the various information obtained from such mean field calculation on the type of stable phase and range of stabilities and construct a global phase diagram.
4. Once such studies are completed we can then use the model potential to design and investigate other desirable properties of liquid crystals.

4. Mean field Theory of Nematic Liquid Crystals

For a nematic phase an order parameter may be defined as a unitless quantity which is nonzero in the nematic phase but vanishes in the isotropic phase for symmetry reasons. Treating the existence of the nematic phase as an order-disorder phenomenon, the expression for the orientational potential energy of a molecule (potential of mean torque) in the nematic phase can be derived in terms of an order parameter [3,10]. The same expression can be derived using the molecular field approximation which is more transparent [3]. The order-disorder theory determines the temperature dependence of an order parameter, calculates the thermodynamic and other properties in terms of the order parameter and demonstrates the precise way in which the transformation from finite value of the order parameter to zero order occurs.

The molecules in the nematic phase of liquid crystals have no translational order. That is the center of mass of the molecules are randomly distributed in space as in any other ordinary liquids. However, they have orientational order, i.e., the rod-like molecules orient their long molecular axis along certain preferred direction on the average. A unit vector used to represent this preferred direction is called director, denoted by \hat{n} .

If the molecules are considered to have a cylindrical symmetry, then just a single order parameter is enough to describe the structure of the nematic phase [3,4,10]. To describe the orientation of a uniaxial molecule, we have used an angle θ between the director and the molecular axis in Fig. 4. If all the molecules are aligned parallel to the director, the angle θ will be zero for all the molecules. On the other hand if there is no preference for a particular

θ , complete isotropy results. The average of the angle θ itself is not a convenient order parameter because commonly the order parameter is always taken such that it is unity in a perfectly ordered phase and is zero in a completely disordered phase. The average of $\cos\theta$, $\langle \cos\theta \rangle$, will vanish in non-ferroelectric nematic phase. If we are not interested in the ferroelectricity, the average of the second order Legendre polynomial $\langle P_2 \rangle$ will be a good order parameter to describe the structure of nematic phase [3,10].

$$\langle P_2 \rangle = \langle \frac{1}{2}(3 \langle \cos^2\theta \rangle - 1) \rangle \quad (1)$$

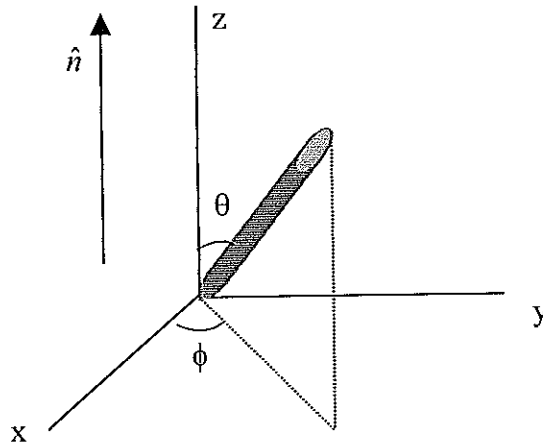


Fig. 4 Coordinate system to define orientation of a uniaxial molecule in a laboratory frame.

According to the mean field approximation, the simplest symmetry allowed orientational potential energy function of a single molecule is given by [3,10]

$$V(\cos\theta) = -\varepsilon \langle P_2 \rangle P_2(\cos\theta) \quad (2)$$

where ε measures the potential well depth. From Fig. 5 we see that the potential is minimum at $\theta=0$ which corresponds to the parallel orientation of the long molecular axis to the director. On the other hand the potential is maximum at $\theta = \pm 90$. This corresponds to perpendicular orientation of the long molecular axis to the director.

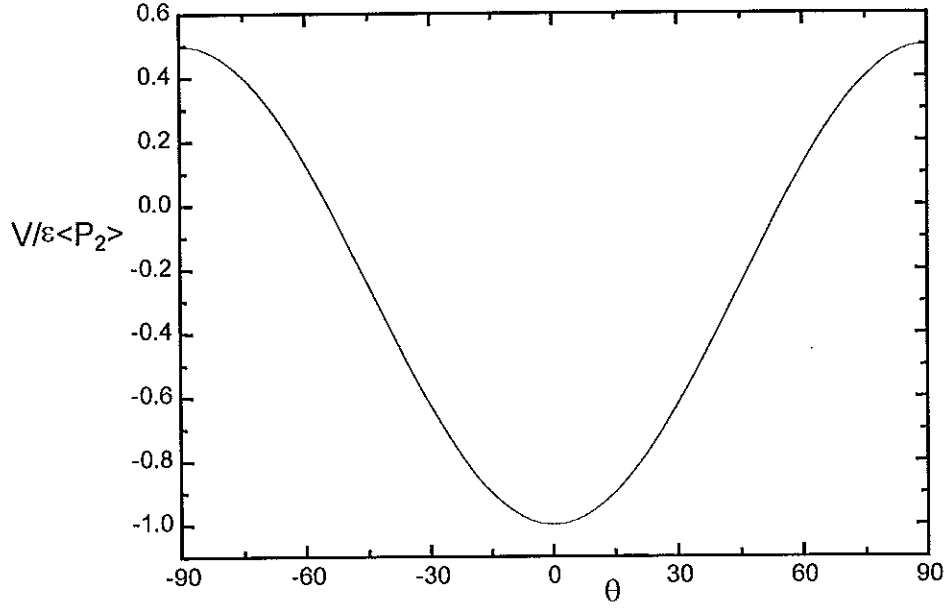


Fig.5 Single molecule orientational potential as a function of the angle θ between the molecular axis and the director.

The average values of various quantities of interest pertaining to the nematic phase can be computed by using the orientational distribution function which is denoted by f . The distribution function is given in terms of the potential function V as [3,10]

$$f(\cos\theta) = \frac{\exp\left[-\frac{1}{kT}V(\cos\theta)\right]}{\int_{-1}^1 \exp\left[-\frac{1}{kT}V(\cos\theta)\right]d(\cos\theta)} \quad (3)$$

where k is the Boltzmann's constant and T is the absolute temperature. The denominator in eq. (3) is represented by the symbol Z and is called the single molecule partition function. The distribution function describes how the molecules are distributed among the possible directions about the director i.e., it gives the probability of finding a molecule at some prescribed angle θ from the director. As we can see from Fig. 6 the distribution function is peaked at $\theta=0$ (for molecules parallel to the director) and becomes very small around $\theta \cong \pi/2$. What is more interesting from Fig. 6 is that the peak decreases as the temperature

increases which implies the decreasing of the degree of order with temperature due to increase of thermal motion of molecules.

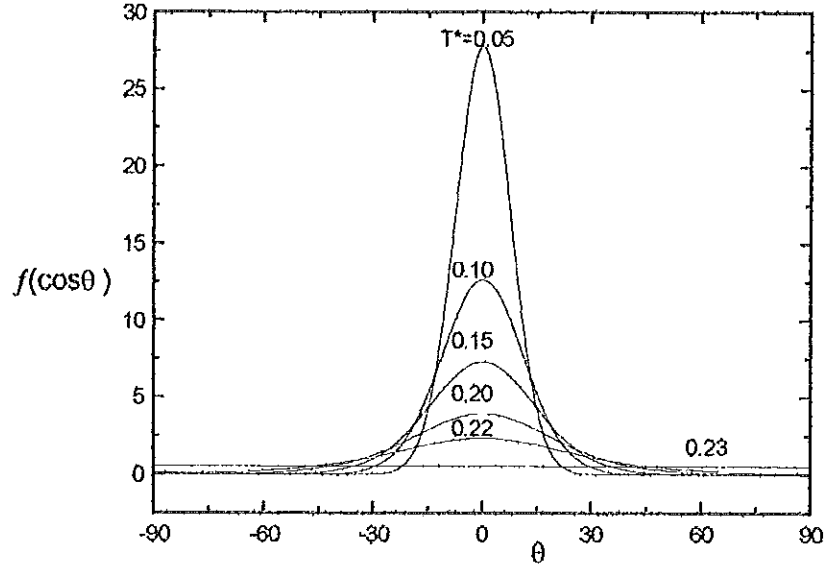


Fig. 6 The orientational distribution function as a function of the angle between the director and the molecular axis at different reduced temperatures, T^* ($T^* = kT/\epsilon$).

In eq.(3) V (and hence f) is a function of $\langle P_2 \rangle$ which is yet undetermined function of temperature. Since $\langle P_2 \rangle$ is the average value of the second Legendre function for a given temperature, its temperature dependence can be determined using eq. (3) as follows [3,10].

$$\langle P_2 \rangle = \int_{-1}^1 P_2(\cos\theta) f(\cos\theta) d(\cos\theta) \quad (4)$$

Substituting the expression for f from eq. (3) we get

$$\langle P_2 \rangle = \frac{\int_{-1}^1 P_2(\cos\theta) \exp\left[\frac{\epsilon}{kT} \langle P_2 \rangle P_2(\cos\theta)\right] d(\cos\theta)}{\int_{-1}^1 \exp\left[\frac{\epsilon}{kT} \langle P_2 \rangle P_2(\cos\theta)\right] d(\cos\theta)} \quad (5)$$

Eq. (5) is called a self-consistent equation for the determination of the temperature dependence of $\langle P_2 \rangle$. For every reduced temperature T^* (where $T^* = kT/\epsilon$) we can use an

iterative procedure to obtain the value of $\langle P_2 \rangle$ that satisfies the self-consistent equation. This has been done by minimizing an error function given by eq. (6).

$$error(\langle P_2 \rangle) = [\langle P_2 \rangle - h(\langle P_2 \rangle)]^2 \quad (6)$$

where

$$h(\langle P_2 \rangle) = \frac{\int_{-1}^1 P_2(\cos \theta) \exp\left[\frac{\varepsilon}{kT} \langle P_2 \rangle P_2(\cos \theta)\right] d(\cos \theta)}{\int_{-1}^1 \exp\left[\frac{\varepsilon}{kT} \langle P_2 \rangle P_2(\cos \theta)\right] d(\cos \theta)}$$

Minimization of the error function was accomplished with the variable metric methods in multidimensions [24] specialized to one dimensional problem. Here, the reason to choose multidimensional minimization program for one dimensional problem is that we want to use the same program for two dimensional problem later on. The FORTRAN program we used for this purpose is given in the appendix.

The result obtained from the program is plotted in Fig. 7. As we can see from the figure the self-consistent equation has three branches of solution. The $\langle P_2 \rangle = 0$ is the solution at all temperatures and corresponds to the isotropic phase. For reduced temperatures T^* below 0.22283, there are two other solutions: the lower and upper branches. The stability of the various phases corresponding to the various solutions will be determined by the orientational free energy evaluated from eq. (12) in the following subsection.

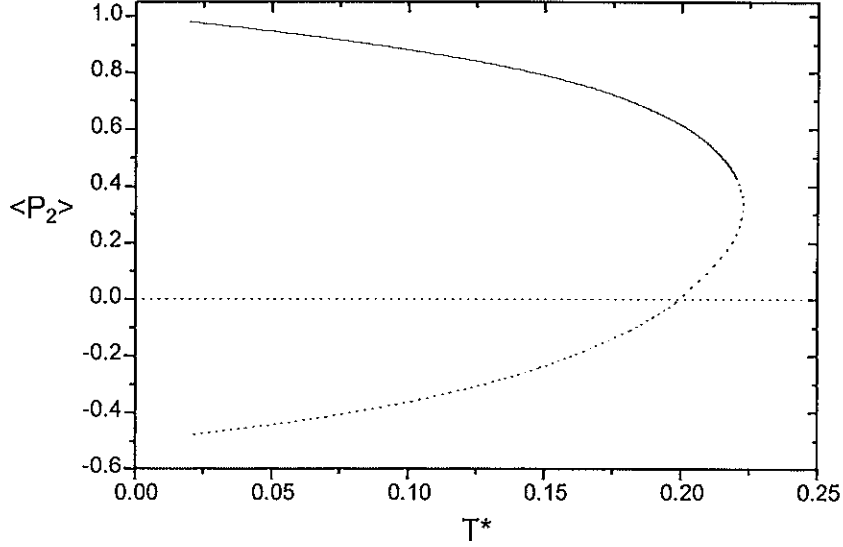


Fig. 7 Temperature dependence of $\langle P_2 \rangle$ obtained by solving the self-consistent equation.

4.1 Thermodynamics of the Nematic Phase

The internal energy E is computed by taking the average value of the potential [3,10].

$$E = \frac{1}{2} N \langle V \rangle \quad (7)$$

where N is the number of molecules and the factor $\frac{1}{2}$ is required to avoid double counting.

The average potential is given by

$$\langle V \rangle = \int_{-1}^1 V(\cos\theta) f(\cos\theta) d(\cos\theta) = -\varepsilon \langle P_2 \rangle^2 \quad (8)$$

Therefore,
$$E = -\frac{\varepsilon}{2} N \langle P_2 \rangle^2 \quad (9)$$

The entropy S is defined as the average value of the logarithm of the distribution function [3,10].

$$S = -Nk \langle \ln f \rangle = -Nk \int_{-1}^1 f \ln f d(\cos\theta) = \frac{N}{T} \langle V \rangle + Nk \ln Z \quad (10)$$

The free energy A is given by

$$A = E - TS \quad (11)$$

Substituting the expression for E and S from eqs. (7) and (10) and rearranging, one can get the following mean field expression for the reduced free energy.

$$A^* = \frac{A}{N\varepsilon} = -T^* \ln Z + \frac{1}{2} \langle P_2 \rangle^2 \quad (12)$$

The free energy for each of the three branches of the order parameter, Fig. 7, was computed from eq. (12). The free energy for the $\langle P_2 \rangle = 0$ branch is constant with temperature and equal to zero. The free energy for the negative $\langle P_2 \rangle$ branch is negative but small in magnitude. The free energy for the positive $\langle P_2 \rangle$ branch is negative up to the transition temperature with magnitude larger than that for the negative $\langle P_2 \rangle$ branch.

The transition temperature was determined by plotting the change in free energy against the reduced temperature, T^* . The order parameter $\langle P_2 \rangle$ is zero in the isotropic phase due to lack of orientational ordering. Consequently, the partition function becomes 2 in the isotropic phase. As a result, the change in free energy is given by

$$\Delta A^*_{NI} = A_I^* - A_N^* = T^* \ln(2/Z) + \frac{1}{2} \langle P_2 \rangle^2 \quad (13)$$

The plot of ΔA^* versus T^* near the transition is shown in Fig. 8. The change in free energy becomes small negative as the temperature increases and is then changed to positive values. In the negative energy region the nematic phase is stable while in the positive region the isotropic phase is stable with vanishing order parameter. The temperature at which the free energy is changed from negative to positive values ($\Delta A^* = 0$) is the nematic to isotropic transition temperature (T^*_{NI}). From the plot T^*_{NI} is equal to 0.22019. The order parameter decreases from unity to a value of 0.4291 at the transition temperature and then vanishes (isotropic phase) as we can see from Fig. 9.

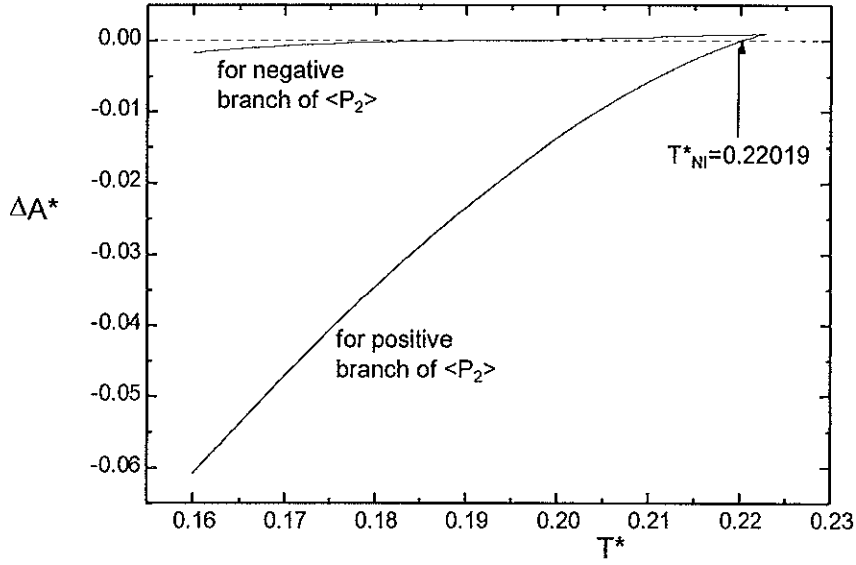


Fig. 8 Temperature dependence of the free energy near the transition.

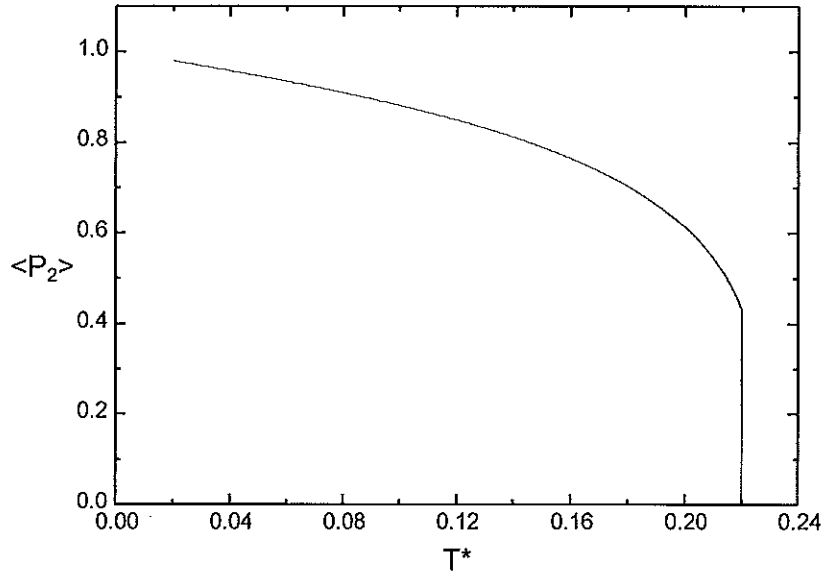


Fig. 9 Plot of equilibrium order parameter as a function of reduced temperature.

Using the transition temperature and the fact that the order parameter changes from 0.4291 to zero at T^*_{NI} , the transition latent heat and the entropy of the transition were calculated.

$$\Delta E_{NI}^* = \frac{\Delta E}{N\varepsilon} = \frac{E_I}{N\varepsilon} - \frac{E_N}{N\varepsilon} = 0 - \left(-\frac{1}{2} \langle P_2 \rangle^2\right) = \frac{1}{2} \langle P_2 \rangle^2 = 0.092 \quad (14)$$

$$\Delta S_{NI}^* = \frac{\Delta S}{Nk} = \frac{\Delta E^*}{T^*} = 0.418 \quad (15)$$

The very small entropy change as compared to solid to liquid phase transition indicates the existence of only very small amount of order in the nematic phase at the transition which is only orientational

The temperature dependence of the heat capacity can be found by numerical differentiation of internal energy versus temperature curve given in Fig. 10 for first and second order phase transitions. The lower curves are first order temperature derivatives of the upper curves.

$$C_V^* = \left(\frac{dE^*}{dT^*} \right)_V \quad (16)$$

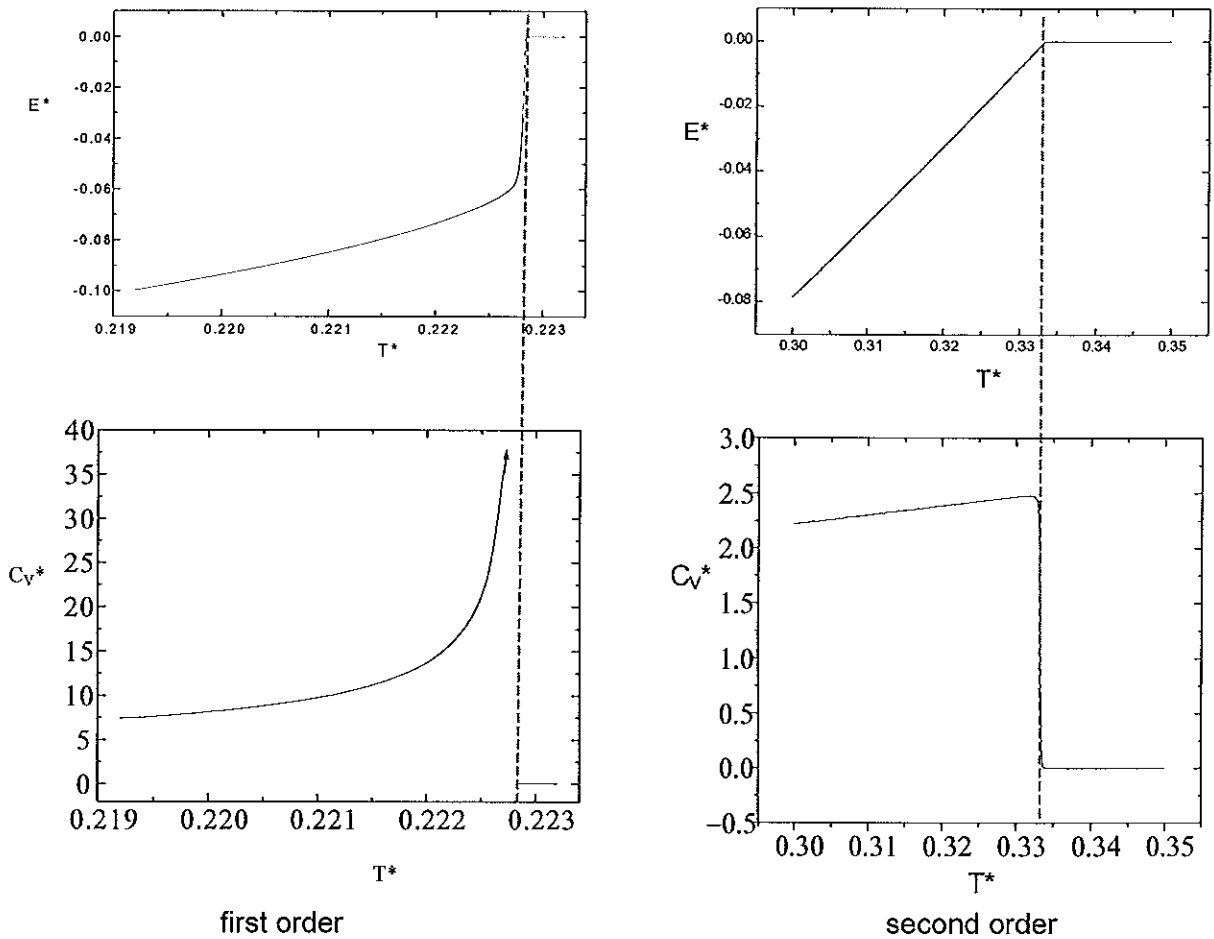


Fig. 10 Behaviour of internal energy and its temperature derivative (heat capacity) for first and second order phase transitions.

Now we can discuss the nature of the nematic to isotropic phase transition using the thermodynamic quantities calculated so far. By using the free energy, the nematic to isotropic transition temperature has been found to be 0.22019 in reduced unit. The transition is first order as the heat capacity (first derivative of the internal energy) shows discontinuity near the phase transition temperature. The arrow on the curve in Fig. 10 for the first order phase transition indicates the divergency of the heat capacity at the transition temperature, i.e., the heat capacity goes to infinity at the transition temperature. However, the heat capacity exhibits discontinuity at a slightly higher temperature than the one we have determined using the free energy. The reason for this is that many properties of the isotropic liquid display critical behaviour on cooling to temperatures close to T_{NI}^* , a phenomenon known as pretransitional behaviour [3,25]. This means the first order phase change to the nematic phase up on cooling takes place just a few degrees before. The smallness of the latent heat and the entropy change at the nematic to isotropic transition is the other reason.

The figure for the second order phase transition is produced using the first rank symmetry allowed potential which corresponds to a pure dipolar interaction and is given in the following section as potential model b. The first rank order parameter obtained from this potential follows second order phase transition.

5. Mean Field Theory of Ferroelectricity in Nematic Liquid Crystals

To study ferroelectricity in nematic liquid crystals a mean field potential containing the lowest symmetry allowed first-rank, second rank and coupling of the two terms was employed. As it has been discussed in section-1, Palffy-Muhoray et al [13] have used an effective single particle potential to study the ferroelectricity in nematic liquid crystals. In our notation their single particle potential may be given as

$$V(\cos\theta) = -c[\delta\{\langle P_2 \rangle \langle P_1 \rangle P_1(\cos\theta) + \langle P_1 \rangle^2 P_2(\cos\theta)\} + \langle P_2 \rangle P_2(\cos\theta)] \quad (17)$$

where $\delta=b/c$, and b and c are constants they have determined and P_i is the i^{th} order Legendere polynomial: the first rank term $P_1(\cos\theta) = \cos\theta$ and the second rank term $P_2(\cos\theta) = 1/2(3\cos^2\theta - 1)$. Their potential, eq. (17), does not contain a pure dipolar interaction term. In addition, they have not investigated the significance of the various terms included in their potential. Here, we include a pure dipolar interaction term in addition to the coupling terms and investigate the significance of the various terms in the potential. The lowest symmetry allowed single particle potential is given as

$$V(\cos\theta) = -\frac{\varepsilon}{V_{\min}}[\lambda \langle P_1 \rangle P_1(\cos\theta) + \delta\{\langle P_1 \rangle \langle P_2 \rangle P_1(\cos\theta) + \langle P_1 \rangle^2 P_2(\cos\theta)\} + \langle P_2 \rangle P_2(\cos\theta)] \quad (18)$$

The first term in eq. (18) considers a pure dipolar interaction and the last term the interaction in ordinary nematic phase. The middle ones are coupling terms. $\langle P_1 \rangle$ will be referred as the ferroelectric order parameter and $\langle P_2 \rangle$ the usual nematic order parameter. The coefficient λ is used for the term without coupling where as δ is used for the coupling terms and they measure the extent of the corresponding interactions. For the purpose of studying the effect of the various terms we have normalized the potential in such a way that the minimum of all

the potentials is minus 1 dividing it by the absolute value of V_{\min} , the minimum values of the potential on the potentials versus orientational angle curve.

By taking out the various terms, the potential given by eq. (18) can be specialized to various potential models. For example, if both λ and δ are zero we will get the potential given by eq. (2) which corresponds to the usual nematic phase. If we ignore the coupling terms, we will end up with a pure dipolar interaction term and a term that stands for the usual nematic phase interaction. The possible combinations of the terms are given below, a-h. Note that potential model a is the same as the potential given by eq. (2) and potential h is the same as eq. (18). Potential e is equivalent to the potential used by the earlier workers [13], eq. (17).

$$V(\cos \theta) = -\varepsilon \langle P_2 \rangle P_2(\cos \theta) \quad (a)$$

$$V(\cos \theta) = -\varepsilon \langle P_1 \rangle P_1(\cos \theta) \quad (b)$$

$$V(\cos \theta) = -\frac{\varepsilon}{V_{\min}} [\delta \langle P_2 \rangle \langle P_1 \rangle P_1(\cos \theta) + \langle P_2 \rangle P_2(\cos \theta)] \quad (c)$$

$$V(\cos \theta) = -\frac{\varepsilon}{V_{\min}} [\lambda \langle P_1 \rangle P_1(\cos \theta) + \langle P_2 \rangle P_2(\cos \theta)] \quad (d)$$

$$V(\cos \theta) = -\frac{\varepsilon}{V_{\min}} [\delta \{ \langle P_2 \rangle \langle P_1 \rangle P_1(\cos \theta) + \langle P_1 \rangle^2 P_2(\cos \theta) \} + \langle P_2 \rangle P_2(\cos \theta)] \quad (e)$$

$$V(\cos \theta) = -\frac{\varepsilon}{V_{\min}} [\delta \langle P_1 \rangle^2 P_2(\cos \theta) + \langle P_2 \rangle P_2(\cos \theta)] \quad (f)$$

$$V(\cos \theta) = -\frac{\varepsilon}{V_{\min}} [\lambda \langle P_1 \rangle P_1(\cos \theta) + \delta \langle P_1 \rangle^2 P_2(\cos \theta) + \langle P_2 \rangle P_2(\cos \theta)] \quad (g)$$

$$V(\cos \theta) = -\frac{\varepsilon}{V_{\min}} [\lambda \langle P_1 \rangle P_1(\cos \theta) + \delta \{ \langle P_2 \rangle \langle P_1 \rangle P_1(\cos \theta) + \langle P_1 \rangle^2 P_2(\cos \theta) \} + \langle P_2 \rangle P_2(\cos \theta)] \quad (h)$$

The orientation dependence of the various potential models at a specific and equal value of λ and δ ($\lambda=\delta=0.65$) is given in Fig. 11. In Fig. 11a, the potential depth of potential a is less

than that of all the other potential models except potential b. This means introducing dipolar interaction to an ordinary nematic phase increases the potential well and hence the stability of the system. Fig. 11b is plotted after all the potentials are divided by the absolute value of their minimum indicated on the dotted lines, i.e., we replot the potentials after they are scaled. As a result in Fig. 11b all the potentials have the same minimum (minus 1) whereas they have four different minimum values in Fig. 11a. The overlapping of some of the potential curves does not mean that the potentials are the same. It is due to our assumption that both $\langle P_1 \rangle$ and $\langle P_2 \rangle$ are equal and unity for the sake of simplicity. The purpose of scaling is to see the significance of the various terms exclusively by avoiding the effect due to the differences in the potential minimum between the various potential models.

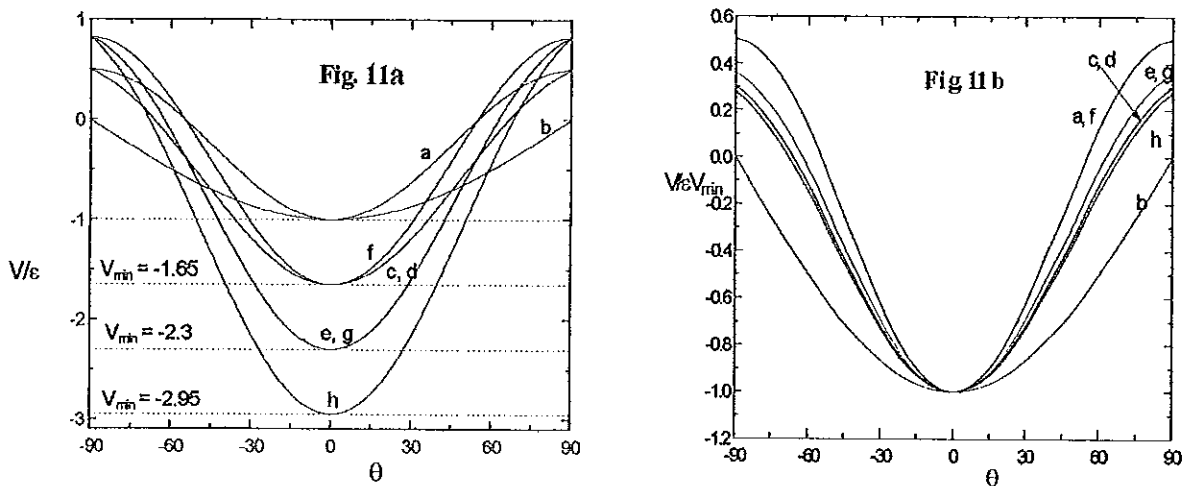


Fig. 11 Orientation dependence of the potentials (a) before normalization and (b) after normalization. For simplicity both $\langle P_1 \rangle$ and $\langle P_2 \rangle$ are taken to be unity.

The coupled self-consistent equations are given as

$$\langle P_1 \rangle = \frac{\int_{-1}^1 P_1(\cos \theta) \exp\left[-\frac{1}{kT} V(\cos \theta)\right] d(\cos \theta)}{\int_{-1}^1 \exp\left[-\frac{1}{kT} V(\cos \theta)\right] d(\cos \theta)} \quad (19)$$

5.1 Effect of Pure Dipolar Interaction on Nematics (potential d)

Here, our strategy is first to study potential d (the potential with pure polar term plus the pure second rank term) exhaustively and then apply the same procedure to the other potential models.

The self-consistent equations were solved for $\langle P_1 \rangle$ and $\langle P_2 \rangle$ by taking an arbitrary value of λ ($\lambda=0.2$). Plotting the two order parameters as a function of reduced temperature on the same graph, the ferroelectric-nematic (FN), nematic (N) and isotropic (I) temperature ranges are shown on the order parameters versus T^* plot (Fig. 12a). Since $\langle P_1 \rangle$ is the ferroelectric order parameter, the temperature at which this order parameter decays to zero is the ferroelectric nematic to nematic transition temperature. The dashed vertical line at $T^* \cong 0.165$ in Fig. 12a indicates this transition reduced temperature. After this temperature, the system becomes normal nematic phase upto the nematic to isotropic transition temperature, the vertical line at $T^*=0.22019$, where $\langle P_2 \rangle$ decays to zero. Once the ferroelectric order parameter, $\langle P_1 \rangle$, decays to zero the value of the usual nematic order parameter, $\langle P_2 \rangle$, obtained from the self-consistent equation using potential d is exactly the same as that obtained using potential a, the potential for the ordinary nematic phase.

If we keep on increasing the value of λ and do the same plot as Fig. 12a, we will get a value of λ at which the nematic region just disappear and only FN and I regions will be observed on the plot, Fig. 12b. At this value of λ the ferroelectricity of the system persists up to a temperature at which the nematic phase is changed to the isotropic phase and hence both $\langle P_1 \rangle$ and $\langle P_2 \rangle$ decay to zero at the same temperature. Since this is the point where the three

phases (FN, N and I) co-exist, the value of λ is called triple point value and denoted by λ_{tr} . This value was determined by varying λ with a step of 0.0001 and solving the self-consistent equations for each value of λ until we got the value where both order parameters decays to zero at the same temperature. By doing this we have found 0.3461 as the triple point value of λ indicated in Fig. 12b.

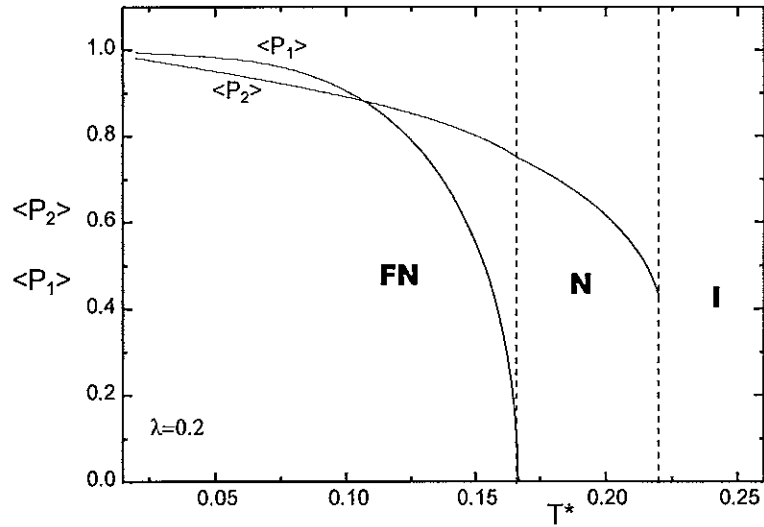


Fig. 12a The ferroelectric -nematic (FN), Nematic (N) and isotropic (I) temperature regions at $\lambda=0.2$

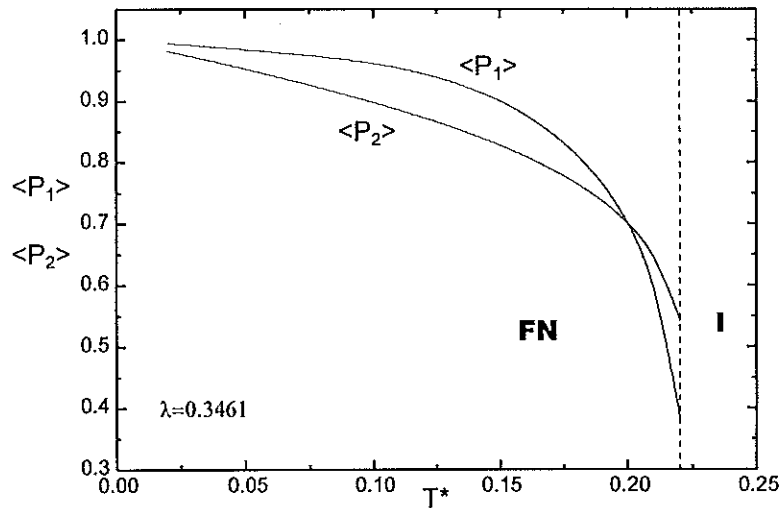


Fig. 12b The FN-N and N-I transition reduced temperatures are equal at $\lambda=0.3461$

As we have discussed above, the self-consistent equations were solved at different values of λ and to show the effect the results that correspond to certain values of λ are plotted in Fig. 13a-b. As we can see from Fig. 13a, for small values of λ , $\langle P_1 \rangle$ decays at lower values of temperature and the ferroelectric-nematic to nematic (FN-N) phase transition is second order. As the values of λ increases the persistence of the ferroelectricity increases and the FN-N phase transition becomes first order. The value of λ at which the FN-N phase transition is changed from second order to first order is called critical value and denoted by λ_c . The critical value has been determined by varying the value of λ with a step of 0.001 and solving the self-consistent equation until we get the value where the phase transition is changed from second order to first order. The nature of the phase transition is more clear from Fig. 13c, $\langle P_1 \rangle$ as a function of $\langle P_2 \rangle$ at different λ values.

In Fig. 13b, the nematic to isotropic (N-I) phase transition temperature is not affected by smaller values of λ , but it starts to increase after certain value of λ . This means strong polar interaction increases the persistence of the nematic phase whereas weak polar interaction has no effect on the N-I transition temperature except increasing the degree of order at low temperature.

Fig. 13c is useful to study the effect of weak and strong dipolar interaction on the ferroelectricity of the nematic phase. At weaker dipolar interaction (smaller values of λ) the ferroelectric order parameter decays to zero while the system is nematic with high degree of order. For instance, for $\lambda=0.1$ the ferroelectricity disappears where the nematic order is about 0.89. For all values of λ less than 0.3461 (triple point value), $\langle P_1 \rangle$ goes to zero before $\langle P_2 \rangle$,

i.e., up on increasing temperature the ferroelectricity disappears before the system is changed from nematic to isotropic phase. For all values of λ greater than or equal to 0.3461 both $\langle P_1 \rangle$ and $\langle P_2 \rangle$ decay to zero at the same temperature and have finite value at the transition temperature. This means for strong dipolar interaction (larger values of λ), the ferroelectricity persists as long as the system is nematic.

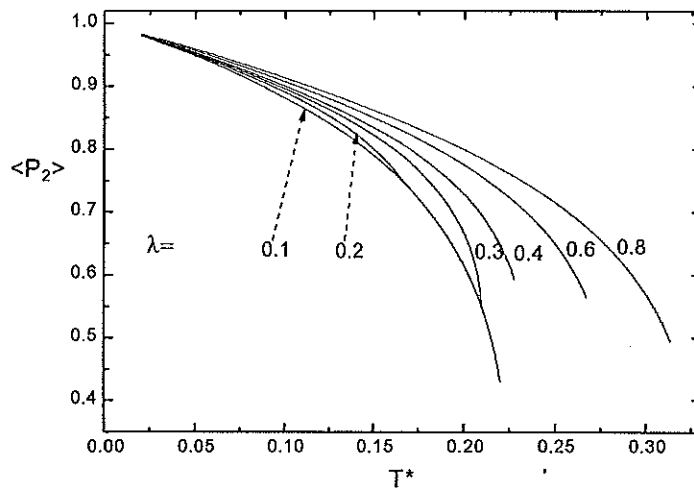


Fig. 13a The dependence of $\langle P_2 \rangle$ on the reduced temperature at different values of λ .

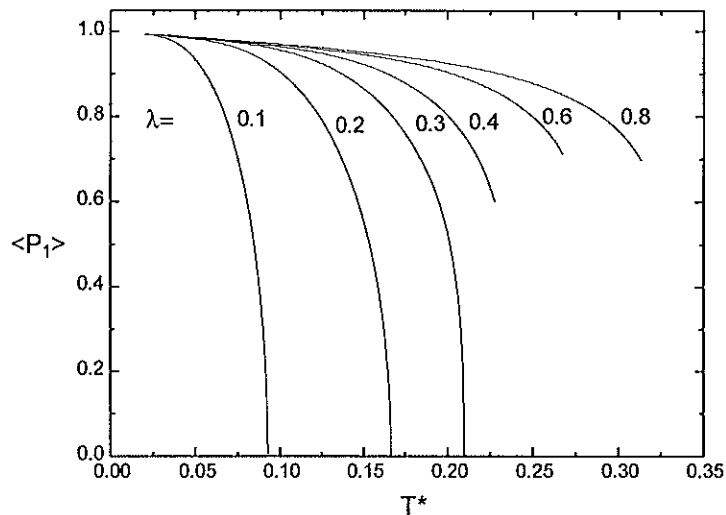


Fig. 13b The dependence of $\langle P_1 \rangle$ and the transition temperature on λ .

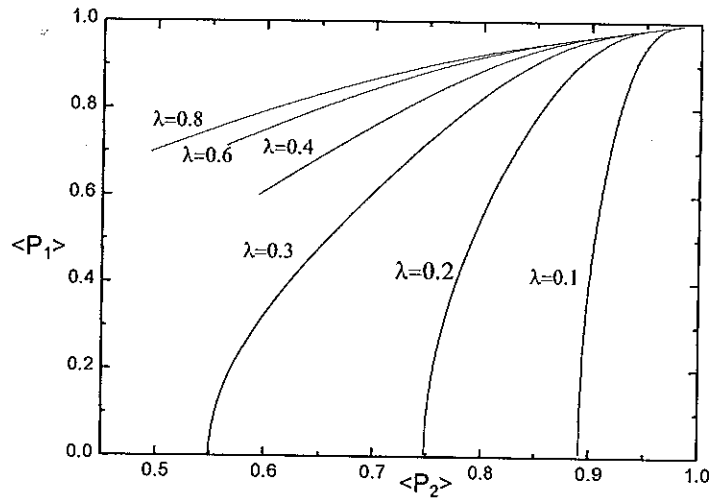


Fig. 13c $\langle P_1 \rangle$ as a function of $\langle P_2 \rangle$ at different values of λ .

From the above discussion, it is clear that the transition temperatures are dependent on the values of λ . Therefore, by plotting reduced temperature as a function of λ , we can have a phase diagram for the chosen potential model as shown in Fig. 14.

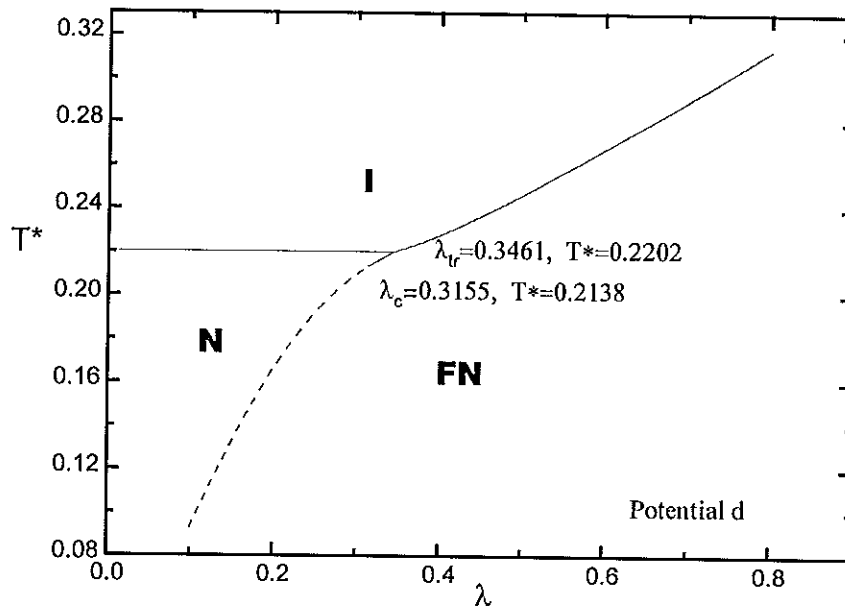


Fig. 14 Phase diagram showing the FN, N and I phases. Solid and dashed lines indicate first and second order phase transitions respectively.

5.2 Effect of Coupling Terms on Nematics (Potentials c, e-g)

The same procedure was repeated for the other potential models as we did for potential d. For potential f the solutions of the self-consistent equations give $\langle P_1 \rangle = 0$ and $\langle P_2 \rangle$ is the same as that obtained in the ordinary nematic phase (potential a) for all values of the coefficients at all reduced temperatures. This is due to lack of first rank variable term in the potential expression. The first rank order parameter, $\langle P_1 \rangle$, obtained from pure dipolar interaction (potential b) follows second order phase transition (Fig. 15b).

The temperature dependence of $\langle P_1 \rangle$ and $\langle P_2 \rangle$, obtained by solving the self-consistent equations using all the other potential models, are plotted on the same graph in Fig. 15a (for $\langle P_2 \rangle$) and 15b (for $\langle P_1 \rangle$). This has been done by taking equal value of λ and δ ($\lambda = \delta = 0.65$) which is greater than the triple point values of all the potential models. The reason for taking a value of the coefficients (λ and δ) greater than the triple point values is to see how the various potential models affect the N-I transition temperature as compared to the normal nematic phase. From the two figures (Figs. 15a and 15b) we may be able to see the effect of introducing the various terms in the potential models on the FN-I transition temperature. In addition to that we can also see how the degree of order is affected for the various potential models.

We can study the figures (Figs. 15a and 15b) by referring to the corresponding expression for the potential models. For instance, by taking out the second term from potential h we get potential g and correspondingly T_{FNI}^* decreases from 0.4383 to 0.3451. Similarly, by taking out the first term from potential h we get potential e and T_{FNI}^* decreases now from 0.4383 to

0.2784. Therefore, we can see that the first term in potential h is more important than the second one for the persistency of the FN phase. This can also be clear by comparing the transition temperatures for potentials c and d. Potential c contains the second and the last terms of potential h while potential d contains the first and the last terms of potential h. As a result of the difference in their first terms, we have transition reduced temperatures of 0.2251 for potential c (potential with coupling term) and 0.2782 for potential d (potential with pure dipolar interaction term). Therefore, from these two arguments it seems that the pure dipolar interaction term has more importance than the second (coupling) term in potential h.

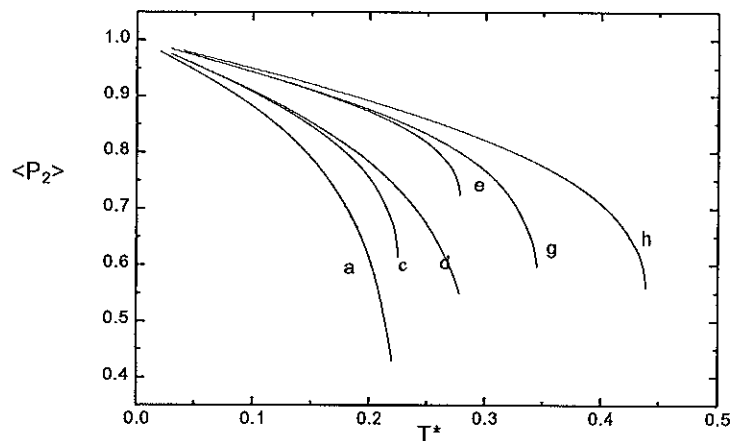


Fig. 15a Temperature dependence of $\langle P_2 \rangle$ obtained from the potential models indicated on the curves for $\lambda = \delta = 0.65$.

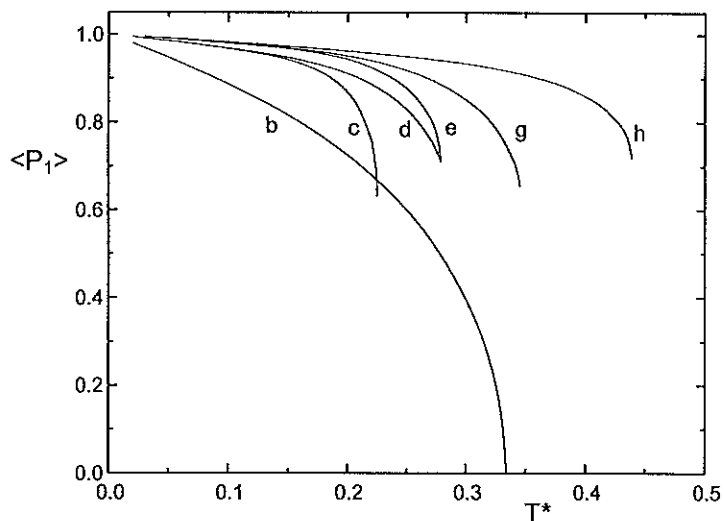


Fig. 15b Temperature dependence of $\langle P_1 \rangle$ obtained from the potential models indicated on the curves for $\lambda = \delta = 0.65$.

In order to avoid the effect of the potential minimum, the potentials are normalized and the temperature dependence of $\langle P_1 \rangle$ and $\langle P_2 \rangle$ are replotted in Figs. 15c and 15d. Because our interest is in the effect of the various terms included in the potential models not in the effect due to the potential minimum. It is interesting to compare the transition temperature for the various potential models in Figs. 15c and 15d. Comparing potential h to potential e in the two figures, we can see how significantly the transition temperature is decreased due to lack of the pure dipolar interaction term in potential e. One thing that seems paradoxical in these figures is that the transition temperature of potential d is even larger than that of potential h which contains all the terms. This may be due to the largest potential minimum scaling factor that results from various terms which does not contribute much to the thermal stability of the system.

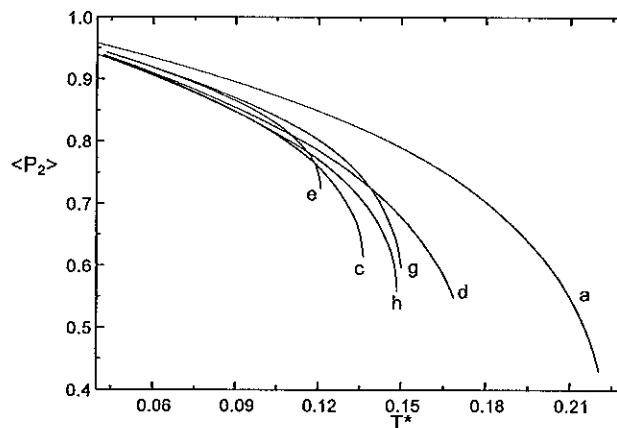


Fig. 15c Temperature dependence of $\langle P_2 \rangle$ after the potentials are normalized.

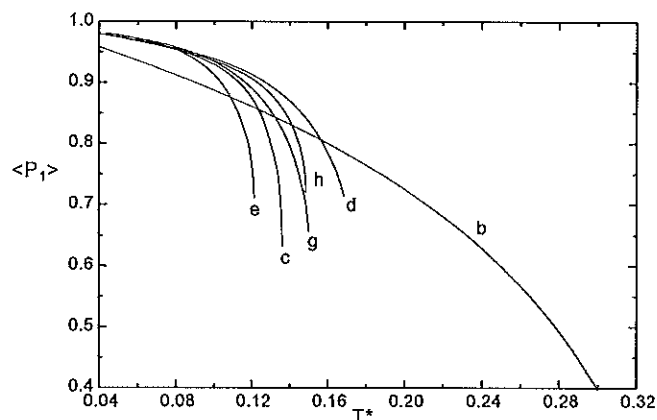


Fig. 15d Temperature dependence of $\langle P_1 \rangle$ after the potentials are normalized.

5.3 Phase Diagrams for the Different Potential Models

As we have done for potential d, we have drawn phase diagrams for the other potential models. We have no phase diagram for potential f as the ferroelectric order parameter obtained from it is zero for all possible values of the coefficient δ at all temperatures. Therefore, potential f is not useful to study ferroelectricity of the system. For potentials c, e, g and h, the self-consistent equations were solved varying the values of λ and δ between 0 and 1. The corresponding phase diagrams are plotted in Fig. 16.

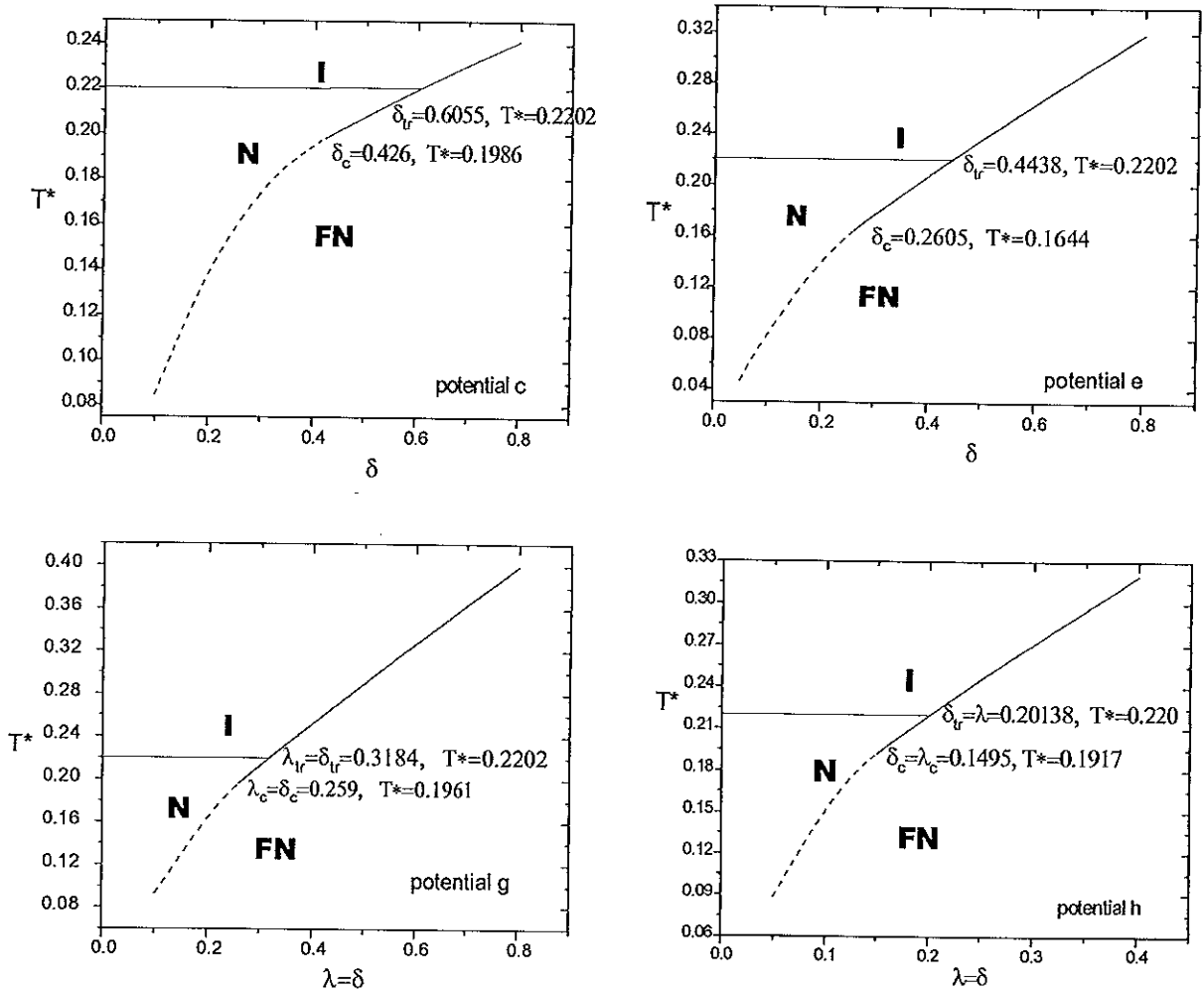


Fig. 16 Phase diagrams showing the FN, N and I phases for the various potential models. Solid and dashed lines indicate first and second order phase transitions respectively.

In Fig. 16 the dashed lines indicate second order phase transition and the solid lines indicate first order phase transitions. As we have discussed in the previous section, the values of λ and δ at which the FN-N phase transition is changed from second order to first order are called critical values and denoted by λ_c and δ_c and the values at the triple point that is the point at which the FN, N and I phases co-exist are called triple point values and denoted by λ_{tr} and δ_{tr} . To determine these critical and triple point values we have followed the same procedure as we have done for potential d. Table I and Table II show the values of the reduced temperature and the order parameters at the critical and triple points for each potential models.

Table I Values of reduced temperature and order parameters at the critical values of λ and δ .

Potential Models	λ_c	δ_c	T^*_c	$\langle P_1 \rangle_c$	$\langle P_2 \rangle_c$
c	-	0.4265	0.1987	0.0	0.6276
d	0.3155	-	0.2138	0.0	0.5249
e	-	0.1605	0.1644	0.0	0.7585
g	0.259	0.259	0.1661	0.0	0.6356
h	0.1495	0.1495	0.1917	0.0	0.6627

Table II Values of reduced temperature and order parameters at the triple point values of λ and δ .

Potential Models	λ_{tr}	δ_{tr}	T^*_{tr}	$\langle P_1 \rangle_{tr}$	$\langle P_2 \rangle_{tr}$
a	-	-	0.2202	-	0.4291
c	-	0.6056	0.2202	0.5819	0.6115
d	0.3461	-	0.2202	0.3794	0.5424
e	-	0.4438	0.2202	0.6080	0.7360
g	0.3184	0.3184	0.2202	0.3962	0.6289
	0.3343	0.1010	0.2202	0.3411	0.5576
	0.3025	0.6625	0.2202	0.4204	0.6924
h	0.20138	0.20138	0.2202	0.4959	0.6449
	0.2417	0.1487	0.2202	0.4539	0.6153
	0.1611	0.2521	0.2202	0.5249	0.6683

The phase diagrams are drawn varying λ and δ equally but Table II includes different triple point values. The purpose of doing this is again to see the significance of the various terms in the potential models. For instance, we can compare the significance of the first (pure dipolar interaction) and the second (coupling) terms in potential g by referring to Table II. Varying λ and δ equally the triple point was obtained at 0.3184. Then λ is increased by 5% and kept as a constant treating δ as a variable to attain the triple point. The 5% increase of λ is compensated by about 68% decrease of δ . Similarly a 5% decrease of λ is compensated by about 108% increase of δ . This clearly shows that the pure dipolar interaction term is significantly more important than the coupling one. This can be further illustrated by referring to the results for potential h in Table II in which 20% increase of λ is compensated by 26% decrease of δ . This means the pure dipolar interaction term has even more influence than the two coupling terms together (the two middle terms in the expression for potential h).

From the discussions so far, we should not conclude that only the pure dipolar interaction term is important without considering the effect of both the pure dipolar and coupling interaction terms on the degree of orders, $\langle P_1 \rangle$ and $\langle P_2 \rangle$. If we look at Table II again for potential models g and h, when we decrease the contribution of the coupling interactions at the expense of the pure dipolar interaction term, the values of both $\langle P_1 \rangle$ and $\langle P_2 \rangle$ at the triple point are smaller than that when λ and δ have equal values. In contrast, when we increase the contribution of the coupling interaction terms, the values of both $\langle P_1 \rangle$ and $\langle P_2 \rangle$ at the triple point are greater than that when λ and δ have equal values. Therefore, the coupling interactions should not be underestimated as they are important for both ferroelectric and normal nematic ordering.

In the phase diagrams the value of the coefficients at the triple point is minimum for potential h and maximum for potential c. From the phase diagrams we also see that the ferroelectric-nematic phase occurs at small value of the coefficients for potential h (note that the coefficients are the measure of the extent of the pure dipolar and coupling interactions). Therefore, although the pure dipolar interaction term seems to be the more important term than the coupling terms, the synergetic effect is more realizable. Because in reality large extent of either interaction may not be available, rather the various interactions contribute some and results in the formation of ferroelectric-nematic phase.

Referring back to the phase diagram for potential d, Fig. 14, we see that the critical point happens to be closer to the triple point. This is due to the significant contribution of the pure first rank term which follows second order phase transition. For potentials c and e the critical point is far away from the triple point as there is no pure first rank term. We have intermediate cases for potentials g and h due to the contributions of both the pure first rank and coupling terms.

References

1. Aldersey-Williams, H., *Electro-Optics*, **1983**, 15, 55.
2. Kelker, H.; Hatz, R., *Handbook of Liquid Crystals*, Velag Chemie, 1980.
3. Priestley, E.B.; Wojtowicz, P.J; Sheng, P., (editors), *Introduction to Liquid Crystals*, Plenum Press: New York and London; 1974.
4. de Gennes, P.G., *The Physics of Liquid Crystals*, Clarendon press: Oxford; 1975.
5. Dekker, A. J. *Solid State Physics*, Prentice-Hall, Inc.; 1961.
6. Fatuzzo, E.; Merz, W.J. *Ferroelectricity*, North-Holland Publishing Company- Amesterdam; 1967
7. Derri, M. *Ferroelectric Ceramics*, Akademiai Kiado, Budapest, 1966.
8. Born, M., *Sitz. Phys. Math.*, **1916**, 25, 614.
9. Chandrasekhr, S., *Liquid Crystals*, Cambridge U.P.; 1977.
10. Lukhurst, G.R., Gray, G.W.(editors), *The Molecular Physics of Liquid Crystals*, Academic Press; 1979.
11. Demus, D., *Liq. Cryst.*, **1989**, 5,75.
12. Luckhurst, G.R. Zannoni, C., *Nature*, Lond.; 1988, 267, 412.
13. Palffy-Muhoray, P., Lee, M.A., Petschek, R.G., *Phys. Rev. Lett.*, **1988**, 60,2303.
14. Madhusudana, N.V., Chandrasekhar, S., *Pramana Suppl.*, **1975**, 1, 57.
15. Sarkar, S., Tough, R. J.A., *J.De Physique*, **1982**, 43,1543.
16. Dunmer, D.A., Toriyama, K., *Liq. Crystals*, **1986**, 1,169.
17. Lee, J.; Ouchi, Y.; Takezoe, H.; Fukuda, A.; Watanabe, J., *J.Phys.: Condens. Matter* **1990**, 2, 275.

18. Skarabot, M.; Cepic, M.; Zeks, B.; Blinc, R.; Heppke, G.; Kityk, V.; Musevic, I., *Physical Review E*, **1998**, 58, 575.
19. Bersnev, L.A., Blinov, L.M., Osipov, M.A., Pikin, S.A., *Mol. Cryst., Liq. Cryst.*, **1988**, 158A, 3.
20. Zentel, R., *Angew. Chem. Advanced Materials.*, **1989**, 101, 321.
21. Vallerien, S.U., Kremer, F., Kapitza, H., Zentel, R., Franck, W., *Phys. Lett. A*, **1989**, 138, 219.
22. Maier, W.; Saupe, A. *Z.Naturforschg.* **1959**, 14a, 882.
23. Maier, W.; Saupe, A. *Z.Naturforschg.* **1960**, 15a, 287.
24. Press, W.H.; Teukolsky, S.A.; Vetterling W.T.; Flannery, B.P. *Numerical Recipes in Fortran*, Cambridge; 1992.
25. Stinson, T.W.; Litster, J.D. *Phys. Rev. Lett.* **1970**, 25, 503.

APPENDIX

**(FORTRAN Program That We Used to Solve
the Self-Consistency Equations)**

```

sum=0.
DO 12 I=1,N
  DO 11 J=1,N
    HESSIN(I,J)=0.
11  CONTINUE
    HESSIN(I,I)=1.
    XI(I)=-G(I)
    sum=sum+p(i)**2
12  CONTINUE
    stpmax=stpmx*max(sqrt(sum),float(n))
    DO 27 ITS=1,ITMAX
      ITER=ITS
      call Lnsrch(n,P,fp,g,xi,pnew,fret,stpmax,check,func)
      FP=FRET
      DO 13 I=1,N
        xi(i)=pnew(i)-p(i)
        p(i)=pnew(i)
13  CONTINUE
        test=0.
        do 14 i=1,n
          temp=abs(xi(i))/max(abs(p(i)),1.)
          if(temp.gt.test)test=temp
14  continue
        if(test.lt.tolx)return
        do 15 i=1,n
          dg(i)=g(i)
15  continue
        CALL DFUNC(P,G)
        test=0.
        den=max(fret,1.)
        do 16 i=1,n
          temp=abs(g(i))*max(abs(p(i)),1.)/den
          if(temp.gt.test)test=temp
16  continue
        if(test.lt.gtol)return
        DO 17 I=1,N
          DG(I)=G(I)-DG(I)
17  CONTINUE
        DO 19 I=1,N
          HDG(I)=0.
          DO 18 J=1,N
            HDG(I)=HDG(I)+HESSIN(I,J)*DG(J)
18  CONTINUE
19  CONTINUE
    FAC=0.
    FAE=0.
    sumdg=0.
    sumxi=0.

```

```

DO 21 I=1,N
  FAC=FAC+DG(I)*XI(I)
  FAE=FAE+DG(I)*HDG(I)
  sumdg=sumdg+dg(i)**2
  sumxi=sumxi+xi(i)**2
21 CONTINUE
  if(fac**2.gt.eps*sumdg*sumxi)then
  FAC=1./FAC
  FAD=1./FAE
  DO 22 I=1,N
    DG(I)=FAC*XI(I)-FAD*HDG(I)
22 CONTINUE
  DO 24 I=1,N
    DO 23 J=1,N
      HESSIN(I,J)=HESSIN(I,J)+FAC*XI(I)*XI(J) &
&      -FAD*HDG(I)*HDG(J)+FAE*DG(I)*DG(J)
23 CONTINUE
24 CONTINUE
  endif
  DO 26 I=1,N
    XI(I)=0.
    DO 25 J=1,N
      XI(I)=XI(I)-HESSIN(I,J)*G(J)
25 CONTINUE
26 CONTINUE
27 CONTINUE
  PAUSE 'too many iterations in DFPMIN'
  RETURN
  END

```

```

subroutine lnsrch(n,xold,fold,g,p,x,f,stpmax,check,func)
logical check
dimension g(n),p(n),x(n),xold(n)
parameter (alf=1.e-4,tolx=1.e-7)
external func
check=.false.
sum=0.
do 11 i=1,n
  sum=sum+p(i)*p(i)
11 continue
sum=sqrt(sum)
if(sum.gt.stpmax)then
  do 12 i=1,n
    p(i)=p(i)*stpmax/sum
12 continue
  endif
slope=0.
do 13 i=1,n

```

```

13      slope=slope+g(i)*p(i)
        continue
        test=0.
        do 14 i=1,n
            temp=abs(p(i))/max(abs(xold(i)),1.)
            if(temp.gt.test)test=temp
14      continue
        alamin=tolx/test
        alam=1.
1      continue
        do 15 i=1,n
            x(i)=xold(i)+alam*p(i)
15      continue
        f=func(x)
        if(alam.lt.alamin)then
            do 16 i=1,n
                x(i)=xold(i)
16      continue
            check=.true.
            return
        else if(f.le.fold+alf*alam*slope)then
            return
        else
            if(alam.eq.1.)then
                tmplam=-slope/(2.*(f-fold-slope))
            else
                rhs1=f-fold-alam*slope
                rhs2=f2-fold2-alam2*slope
                a=(rhs1/alam**2-rhs2/alam2**2)/(alam-alam2)
                b=(-alam2*rhs1/alam**2+alam*rhs2/alam2**2/ &
                    (alam-alam2)
                if(a.eq.0.)then
                    tmplam=-slope/(2.*b)
                else
                    disc=b*b-3.*a*slope
                    tmplam=(-b+sqrt(disc))/(3.*a)
                endif
                if(tmplam.gt..5*alam)tmplam=.5*alam
            endif
        endif
        alam2=alam
        f2=f
        fold2=fold
        alam=max(tmplam,.1*alam)
        goto 1
    end

```

```

function func(p)
!func is the error function to be minimized.
dimension p(2)
external fn,gn,zn
call qromb(fn,-1.0,1.0,f1)
call qromb(gn,-1.0,1.0,f2)
call qromb(zn,-1.0,1.0,f3)
p1c=f3/f2
p2c=f1/f2
func=(p(1)-p1c)**2+(p(2)-p2c)**2
return
end

subroutine dfunc(p,g)
!dfunc is the gradient (derivative) of func.
dimension p(2),g(2)
external fn,gn,zn
call qromb(fn,-1.0,1.0,f1)
call qromb(gn,-1.0,1.0,f2)
call qromb(zn,-1.0,1.0,f3)
p1c=f3/f2
p2c=f1/f2
g(1)=2.0*(p(1)-p1c)
g(2)=2.0*(p(2)-p2c)
return
end

SUBROUTINE QROMB(FUNC,A,B,SS)
!This subroutine is used to integrate a given function.
PARAMETER (EPS=1.E-6,JMAX=20,JMAXP=JMAX+1,K=5,KM=4)
DIMENSION S(JMAXP),H(JMAXP)
H(1)=1.
DO 11 J=1,JMAX
  CALL TRAPZD(FUNC,A,B,S(J),J)
  IF (J.GE.K) THEN
    L=J-KM
    CALL POLINT(H(L),S(L),K,0.,SS,DSS)
    IF (ABS(DSS).LT.EPS*ABS(SS)) RETURN
  ENDIF
  S(J+1)=S(J)
  H(J+1)=0.25*H(J)
11 CONTINUE
return
END

SUBROUTINE POLINT(XA,YA,N,X,Y,DY)
PARAMETER (NMAX=10)
DIMENSION XA(N),YA(N),C(NMAX),D(NMAX)

```

```

          X=X+DEL
11      CONTINUE
          S=0.5*(S+(B-A)*SUM/TNM)
          IT=2*IT
      ENDIF
      RETURN
      END

```

```

function zn(x)
dimension p(2)
common/order/p
common/temp/rt
common/lamda/rl
common/delta/d
p1x=x
p2x=1.5*x**2-0.5
V=rl*p(1)*p1x+d*(p(1)*p(2)*p1x+p(1)**2*p2x)+p(2)*p2x
!V is potential model h and to use this program for the other
!potential models you only need to change this expression.
zn=p1x*exp(V/rt)
return
end

```

```

function fn(x)
dimension p(2)
common/order/p
common/temp/rt
common/lamda/rl
common/delta/d
p1x=x
p2x=1.5*x**2-0.5
V=rl*p(1)*p1x+d*(p(1)*p(2)*p1x+p(1)**2*p2x)+p(2)*p2x
fn=p2x*exp(V/rt)
return
end

```

```

function gn(x)
dimension p(2)
common/order/p
common/temp/rt
common/lamda/rl
common/delta/d
p1x=x
p2x=1.5*x**2-0.5
V=rl*p(1)*p1x+d*(p(1)*p(2)*p1x+p(1)**2*p2x)+p(2)*p2x
gn=exp(V/rt)
return
end

```